

RESEARCH

Open Access

Aldose reductase from *Schistosoma japonicum*: crystallization and structure-based inhibitor screening for discovering antischistosomal lead compounds

Jian Liu^{1,2}, David H Dyer³, Jingdong Cheng⁴, Jipeng Wang², Shuqi Wang², Zhong Yang², Xiaoning Wang² and Wei Hu^{1,2*}

Abstract

Background: Schistosomiasis is a neglected tropical disease with high morbidity and mortality in the world. Currently, the treatment of this disease depends almost exclusively on praziquantel (PZQ); however, the emergence of drug resistance to PZQ in schistosomes makes the development of novel drugs an urgent task. Aldose reductase (AR), an important component that may be involved in the schistosome antioxidant defense system, is predicted as a potential drug target.

Methods: The tertiary structure of *Schistosoma japonicum* AR (SjAR) was obtained through X-ray diffraction method and then its potential inhibitors were identified from the Maybridge HitFinder library by virtual screening based on this structural model. The effects of these identified compounds on cultured adult worms were evaluated by observing mobility, morphological changes and mortality. To verify that SjAR was indeed the target of these identified compounds, their effects on recombinant SjAR (rSjAR) enzymatic activity were assessed. The cytotoxicity analysis was performed with three types of human cell lines using a Cell Counting Kit-8.

Results: We firstly resolved the SjAR structure and identified 10 potential inhibitors based on this structural model. Further *in vitro* experiments showed that one of the compounds, renamed as AR9, exhibited significant inhibition in the activity of cultured worms as well as inhibition of enzymatic activity of rSjAR protein. Cytotoxicity analysis revealed that AR9 had relatively low toxicity towards host cells.

Conclusions: The work presented here bridges the gap between virtual screening and experimental validation, providing an effective and economical strategy for the development of new anti-parasitic drugs. Additionally, this study also found that AR9 may become a new potential lead compound for developing novel antischistosomal drugs against parasite AR.

Keywords: *Schistosoma japonicum*, Aldose reductase (AR), Structure, Virtual screening, Drug target

* Correspondence: huwyz@163.com

¹Key Laboratory of Parasite and Vector Biology of MOH, Institute of Parasitic Diseases, Chinese Center for Disease Control and Prevention, 207 Rui-Jin Road II, Shanghai 200025, China

²Department of Microbiology and Microbial Engineering, School of Life Sciences, Fudan University, 220 Han-Dan Road, Shanghai 200433, China
Full list of author information is available at the end of the article

Background

Schistosomiasis is a major tropical disease in developing countries. It is estimated that over 200 million people from 76 countries and territories are suffering from this disease [1]. The disease is usually caused by one of three schistosome species: *Schistosoma japonicum*, *Schistosoma mansoni* and *Schistosoma haematobium*. In China, *S. japonicum* is the primary pathogen of this disease [2]. Currently, the treatment of schistosomiasis depends almost exclusively on praziquantel (PZQ), and this drug has been widely used for nearly 40 years because of its high efficacy but low cost [3]. However, the long-term utilization of one drug can result in drug-resistant parasites. Decreased susceptibility of *S. mansoni* and *S. haematobium* to PZQ has already been identified in previous studies [4,5]. Although no reduced susceptibility of *S. japonicum* has been proven to date, the efficacy of this drug is found to vary in different strains within this species [6]. Therefore there is an urgent need to develop novel antischistosomal lead compounds, and the identification of ideal drug targets is an important step toward this goal.

Antioxidant defense is an essential mechanism for schistosomes to cope with damage from host immune- and self-generated reactive oxygen species (ROS) [7]. Many redox-associated proteins such as thioredoxin glutathione reductase (TGR), peroxiredoxin (Prx) and thioredoxin (Trx) have been demonstrated to be involved in this system in previous studies [8-11]. Most of these proteins are considered as potential drug targets, as one example, two recently discovered prospective antischistosomal compounds, auranofin and oxadiazoles, were developed with TGR as drug target [9,12]. Although no research has shown that *S. japonicum* AR participates in the antioxidant pathway, in other organisms, AR is believed to be an important antioxidant component. Spycher *et al.* [13] found that the levels of AR mRNA were up-regulated under oxidative stress in rat smooth muscle cells. Furthermore, the levels of AR expression as well as its activity were increased during hyperglycemia and other oxidative stress-induced diseases in humans [14,15]. Additionally, many byproducts of oxidative stress, such as methylglyoxal and 3-deoxyglucosone, have been shown to be excellent substrates of AR [16]. Considering both these conclusions and the antioxidant requirement of schistosomes, it is reasonable to speculate that *SjAR* might also participate in the antioxidant pathway and protect the worms from host ROS attack. In addition to the above, AR has also been demonstrated to play an important role in aldehyde detoxification, steroid metabolism, energy supply, cellular proliferation, apoptosis and senescence [17-20]. Its multiple functions suggest that it may represent a key enzyme in schistosomes.

In the present study, we successfully resolved the tertiary structure of recombinant *SjAR* and identified 10

inhibitor candidates through molecular docking based on the obtained structural model. We then assessed the activity inhibition of these compounds on cultured worms. To further confirm that the *SjAR* protein was indeed the target of the selected compounds, we investigated the effect of the identified compounds on the enzymatic activity of recombinant *SjAR* (r*SjAR*). The cytotoxicity of the active compounds towards the host cell was evaluated as well. Finally, one compound, renamed as AR9, was determined to effectively inhibit the activity of cultured worms but show relatively low cytotoxicity against host cells, which suggests its potential use as a lead compound from the selected candidate inhibitors. The work presented here bridges the gap between virtual screening and experimental validation, providing an effective and economical strategy to develop novel anti-parasitic drugs.

Methods

Materials

Protein crystallization kits were purchased from Hampton Research Corporation (USA). NADPH was obtained from Roche (Switzerland). DL-glyceraldehyde and PZQ came from Sigma (USA). Small molecules identified by virtual screening were purchased from Maybridge HitFinder library (USA). RPMI 1640, DMEM and bovine serum (Newborn calf serum and fetal bovine serum) came from Invitrogen (USA). The recombinant *SjAR*-pET28a plasmid was constructed previously and stored in our laboratory. BL21 (DE3) and Hep G2 cells were also stored in our laboratory. 293T and HeLa cell lines were kindly provided by Hongyan Wang (School of Life Sciences, Fudan University, China). *S. japonicum* cercaria was provided by the pathogen biology laboratory of the National Institute of Parasitic Diseases, Chinese Center for Diseases Control and Prevention. Specific pathogen-free Kunming female mice were purchased from the Shanghai Experimental Animal Center, Chinese Academy of Sciences (China).

Expression and purification of r*SjAR*

The recombinant plasmid *SjAR*-pET28a was transformed into *E. coli* BL21 (DE3) cells and cultured in Luria-Bertani (LB) medium plus 50 µg/ml kanamycin. Isopropylthio-β-D-galactoside (IPTG), 1 mM, was added to the medium to induce protein expression, and then the cells were cultured for an additional 6 h. The cells were harvested by centrifugation, and pellets were resuspended in lysis buffer (20 mM Tris-HCl, 500 mM NaCl, 1 mM PMSE, pH 8.0). Subsequently, the cells were disrupted by ultrasonic waves for 5 min in 2 s pulses at 160 W. The whole cell lysate was clarified by centrifugation at 10,000 × *g* for 30 min at 4°C. The resulting supernatant was purified sequentially using immobilized metal ion affinity chromatography, anion-exchange

chromatography, and finally, size-exclusion chromatography. The purified protein was stored in 20 mM Tris-HCl (pH 6.2), 100 mM NaCl, 5 mM DTT. The rSjAR protein was concentrated by ultrafiltration using Millipore Ultrafiltration System with a molecular weight cut off at 10 KDa. Protein concentration was determined by a Bradford Protein Assay Kit (Glory, USA).

Crystallization

Initial crystallization conditions were screened in Tissue Culture Test Plates 24 (TPP) by the hanging-drop method at 291 K, using the sparse-matrix method [21] implemented in the Crystallization Screens Kits (included Index, Crystal Screen, Crystal Screen 2, PEG/Ion Screen and PEG/Ion 2 Screen and SaltRx) from Hampton Research. Three protein concentrations were adopted: 24 mg/ml, 12 mg/ml and 6 mg/ml. A total of 1 μ l protein solution was mixed with 1 μ l well solution and equilibrated against 200 μ l reservoir solution. Crystallization leads were identified in over 10 of these conditions. One initial condition (PEG/Ion Screen: 0.2 M Sodium fluoride, 20% w/v Polyethylene glycol 3,350, pH 7.3), which produced single crystals, was optimized to obtain crystals suitable for diffraction analysis. The final optimal conditions were 12 mg/ml protein and a reservoir solution consisting of 0.2 M Sodium fluoride, 30% w/v, Polyethylene glycol 3,350 (pH 7.1).

Data collection and processing

Crystals were flash-cooled in liquid nitrogen with a cryoprotectant containing only reservoir solution. Diffraction data were collected at Beamline BL17U at the Shanghai Synchrotron Radiation Facility and processed with the package HKL-2000 using routine procedures [22]. The initial phases were calculated in the program PHASER [23], from the CCP4 suites, using a structure known *H. sapiens* AR (*HsaAR*, PDB ID: 1ZUA) as a search model. The final model was manually built with COOT [24]. All computational refinements were performed using the refinement module phenix.refine of the PHENIX package [25]. The model quality was checked with the PROCHECK program, which showed good stereochemistry according to the Ramachandran plot for the structure.

Molecular docking

To identify potential inhibitors of SjAR, the Maybridge HitFinder library, which contains approximately 80,000 compounds, was chosen for *in-silico* screening with the model of the rSjAR protein. Molecular docking was firstly performed with Sybyl v8.0 Surfex-Dock (www.tripos.com) followed by docking the top 5% hits with AutoDock 4.2 (http://autodock.scripps.edu/). The top 100 scoring compounds were selected out and exported to an Excel spreadsheet. To increase the selectivity of these compounds, they

were also docked into the *HsaAR* protein. The final obtained compounds conformed to the following principles: 1) the SjAR protein-compound binding free energy was lower than -9 kCal/mol; and 2) the compound showed a greater binding preference to the SjAR protein than to *HsaAR* (the difference of binding free energy was higher than 2 kCal/mol).

Inhibition studies on cultured worms

Mice infected with 80–100 cercariae were killed at 35 days-post-infection for worm collection. *S. japonicum* adult worms were obtained by perfusion and washed three times with sterile saline. Next, the worms were transferred to RPMI 1640 medium containing 300 μ g/ml penicillin, 300 μ g/ml streptomycin, 0.25 μ g/ml amphotericin and 20% fetal bovine serum and then cultured for 2 h to make the worms discharge their gut contents. Two pairs of worms with good activity were selected and transferred to each well of a 24-well plate containing 2 ml of the preceding culture medium. Stocking solutions of compounds were prepared by dissolving 2 mg of the compounds in 0.4 ml dimethyl sulfoxide (DMSO) and then were added to a series of final concentrations (for initial screening, three concentrations of 5 μ g/ml, 25 μ g/ml and 50 μ g/ml were assessed, while for the second screening, five concentrations of 1.25 μ g/ml, 2.5 μ g/ml, 5 μ g/ml, 10 μ g/ml, and 20 μ g/ml were assessed). The worms in the control group were treated with equal amounts of the compound carrier. A PZQ treated group was also observed as a positive control. The test was repeated three times, and for each experimental condition, 12 worms in 3 wells were tested.

The worms were cultured at 37°C in an incubator with 5% CO₂. The worm mobility, morphological changes and mortality were observed under an inverted microscope at 2 h, 24 h, 48 h and 72 h. Parasite death was defined as non-detectable activity in 2-minutes, accompanied by morphological and tegumental alterations [26]. The median lethal concentration (LC50) values for the identified active compounds were calculated by the software SPSS 18.0, with a confidence interval of 95%.

Effect of compound AR9 on rSjAR enzymatic activity

The enzymatic assay was described previously [27]. Briefly, the reaction was performed in 120 mM PBS buffer (pH 6.2), containing 1.5 mM DL-glyceraldehyde, 0.15 mM NADPH and 0.15 μ M rSjAR in a final volume of 200 μ l. The mixture was first incubated at 37°C for 5 min, and then the reaction was initiated by adding the substrate of NADPH. For inhibition analysis, AR9 was added to the same reaction system to final concentrations of 5 μ g/ml, 10 μ g/ml, 20 μ g/ml and 40 μ g/ml. The reaction process was determined by monitoring the absorbance reduction at 340 nm due to the depletion of NADPH using a Model 680 Microplate Reader (Bio-Rad, USA).

Table 1 X-ray data-collection and structure refinement statistics

Data collection and processing	
Processing software	HKL2000
Synchrotron, beamline	SSRF, BL17U
Wavelength (Å)	0.9791
Space group	P2 ₁ 2 ₁ 2
Unit cell parameters a, b, c (Å, °)	a = 67.49, b = 91.00, c = 54.67
Resolution range (Å) ¹	30.0-2.20 (2.28-2.20)
Unique reflections	17617
Redundancy	6.4 (6.5)
Completeness (%)	99.8 (99.9)
R _{merge} (%)	12.5 (37.1)
I/σ(I)	13.8 (5.0)
Refinement statistics	
Refinement software	PHENIX
R _{work} (%) / R _{free} (%) ²	17.7 / 21.7
Average B factor, (Å ²)	17.9
RMSD from ideal geometry, bonds (Å)	0.007
RMSD from ideal geometry, angles (°)	1.023
Protein atoms	2452
Water molecules	225
Residues in the Ramachandran plot	
Most favored region (%)	92.5
Allowed region (%)	7.5
Generously allowed region (%)	0
Disallowed region (%)	0

¹Values in parentheses are for the highest resolution shell.

² $R_{free} = \frac{\sum_{Test} |F_{obs}| - |F_{calc}|}{\sum_{Test} |F_{obs}|}$, where "Test" is a test set of about 5% of the total reflections randomly chosen and set aside before refinement.

Scanning electron microscopy (SEM)

Schistosome samples were fixed with 2.5% glutaraldehyde in PBS buffer for 2 h and were then washed thoroughly three times with PBS buffer. The samples were fixed again in 1% osmium tetroxide in PBS buffer. After ethanol dehydration and critical point drying, they were mounted on microscope stubs, followed by gold sputtering for 3 min in an IB-3 ion-sputtering instrument. The SEM scanning was performed on an S-520 SEM (Hitachi, Japan) instrument with an accelerating voltage of 20 kV [28].

Cytotoxicity assay

Cytotoxicity analysis was performed with three types of human cell lines (Hep G2, 293T and Hela cell lines) using a Cell Counting Kit-8 according to the protocol provided by the manufacturers (Beyotime, China). Briefly, the cells were cultured in a 96-well plate containing 100 μl DMEM medium (containing 10% fetal bovine serum) at a density of 5,000 cells per well at 37°C in 5% CO₂. The cells were allowed to recover for 24 h and then exposed to various concentrations of compound or compound-carrier. When the cells in the negative control group (carrier alone) covered more than 90% of the surface of the well, 10 μl of WST-8 chromogenic agent was added to each well and then continuously incubated for 30 min. The absorbance at 450 nm was determined by using a Model 680 Microplate Reader (Bio-Rad, USA).

Ethical approval

The animal work was approved by the Ethics Committee of the National Institute of Parasitic Diseases, Chinese Center for Disease Control and Prevention in Shanghai, China (Ref No: 20100525-1). Animal care and all procedures involving animals were performed in strict accordance with the Guidelines for the Care and Use of Laboratory Animals of the Ministry of Science and Technology of People's Republic of China ([2006]398). All efforts were made to minimize suffering.

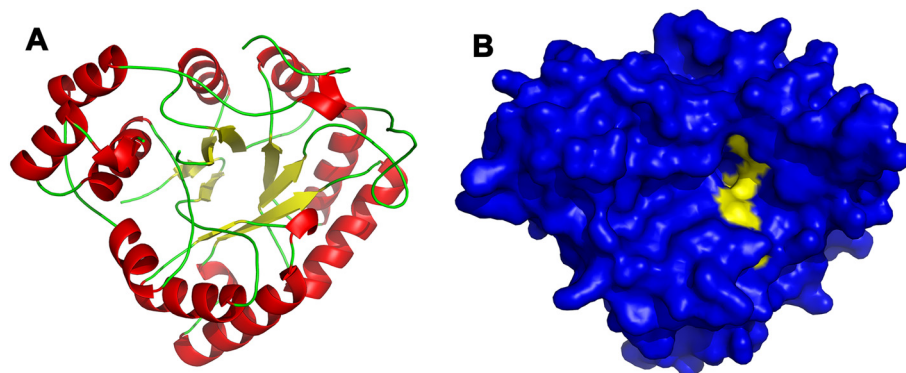


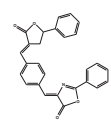
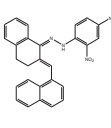
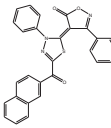
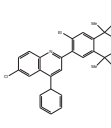
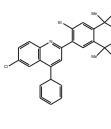
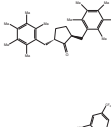
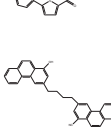
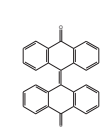
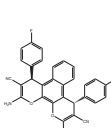
Figure 1 Structure and predicted cofactor binding area of the SjAR protein. **A.** Cartoon diagram of SjAR with α-helices colored red, β-sheets colored yellow and loops colored green. **B.** The structure of SjAR is shown in a surface representation with the regions predicted to be involved in cofactor binding (by homology with *H. sapiens* AR) colored yellow.

Results

Structure determination and description

The rSjAR protein crystals diffracted to a resolution of 2.2 Å and belonged to the space group P2₁2₁2 with the unit cell parameters a = 67.49, b = 91.00 and c = 54.67 Å.

Table 2 The finally obtained 10 candidate compounds analyzed with AutoDock 4.2

Compound ID	Structure	Binding free energy (kCal/mol)		SjAR-HsaAR (kCal/mol)
		SjAR	HsaAR	
AR1		-13.56	-11.42	2.14
AR2		-13.80	-10.61	3.19
AR3		-12.77	-10.47	2.30
AR4		-10.09	-6.09	4.00
AR5		-11.59	-9.52	2.07
AR6		-9.31	-7.00	2.31
AR7		-9.05	-6.34	2.71
AR8		-13.47	-10.99	2.48
AR9		-10.08	-8.07	2.01
AR10		-9.15	-3.78	5.37

Residues 211–221 were disordered and were not built into the structure model. After structure solution and computational refinement, the final model of SjAR, validated using PROCHECK, had 92.5% of residues in the most favored regions of the Ramachandran plot and 7.5% of residues in the additionally allowed regions. The structure had Root Mean Square Deviation (RMSD) from ideality for bond lengths of 0.007 Å and for an angle of 1.023°. Further data collection and computational refinement statistics are summarized in Table 1.

The overall structure of SjAR (PDB ID: 4HBK) showed an (α/β)₈ barrel topology, which is the typical characteristic of the aldo-keto reductase superfamily (Figure 1A) [29,30]. By comparing the amino acid sequence with the homologous HsaAR protein, we found both the residues at the substrate-binding site (Asp⁴³, Tyr⁴⁸, Lys⁷⁷ and His¹¹⁰) and at the predicted inhibitor-binding sites (Tyr⁴⁸, His¹¹⁰ and Trp¹¹¹) were conserved [30,31]. These residues were located in the interior of the β-barrel, which provided a target area to begin docking (Figure 1B).

Structure-based virtual screening

Although the SjAR protein shares only 51% sequence identity with HsaAR (PDB ID: 1ZUA), their tertiary structures are highly similar (RMSD: 0.865 Å). The AR protein family has highly conserved substrate binding sites, and all the nearby residues surrounding the binding sites are the same, which suggests that the region would be somewhat unsuitable for docking. Therefore, we compared the structural divergence near the potential inhibitor binding regions. Compared with the known HsaAR-tolrestat complex structure [30], in the SjAR structure, Lys²⁵⁷ penetrated into the binding regions, while Gln²⁹⁷ and Trp²⁰ were moved away. Additionally, Phe²⁹³ replaced Cys²⁹⁹ to participate in the formation of the hydrophobic pocket. However, all of these residues

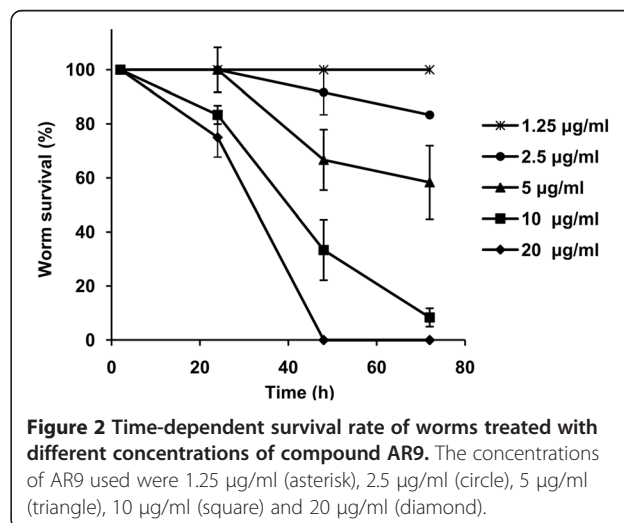


Figure 2 Time-dependent survival rate of worms treated with different concentrations of compound AR9. The concentrations of AR9 used were 1.25 µg/ml (asterisk), 2.5 µg/ml (circle), 5 µg/ml (triangle), 10 µg/ml (square) and 20 µg/ml (diamond).



Figure 3 Observation of worms exposed to compound AR9 under optical microscopy. **A.** Worms treated with 5 µg/ml of AR9 for 48 h; **B.** treatment with 10 µg/ml of AR9 for 72 h; **C.** Positive control group, treatment with 5 µg/ml of PZQ for 48 h; **D.** Negative control, treatment with AR9 carrier only for 72 h.

had the potential to interact with inhibitors. The finally obtained 10 candidate compounds as well as their binding free energy with *SjAR* and *HasAR* were listed in Table 2.

Inhibition studies on cultured worms

The effects of the identified compounds on adult worms were observed by culturing the worms in medium containing different amounts of each compound, and death rates as well as morphological alterations were

monitored. In the primary screening, two compounds, AR6 and AR9, exhibited good inhibition ability on cultured worms. AR6 resulted in 75% mortality after 72 h, but the effect was limited to 50 µg/ml. A similar effect was observed for AR9 with activity at a lower concentration; thus, it was selected for the secondary screening to confirm the efficacy of AR9 and further determine its LC50 value. Here, 10 µg/ml of AR9 resulted in 91.67% mortality over 72 h, and at 20 µg/ml, 100% mortality over 48 h was observed. In contrast, worms treated with equal volume of DMSO maintained a good activity throughout the whole experimental period (Figure 2).

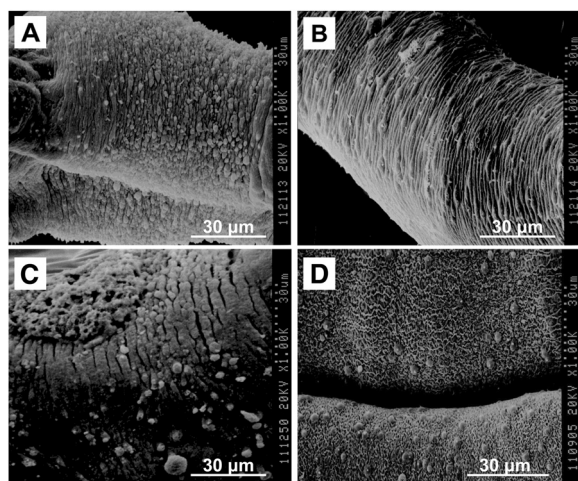


Figure 4 SEM images of the tegument of adult worms. **A** and **B** were worms treated with 10 µg/ml of AR9; **C.** Positive control group, treated with 10 µg/ml of PZQ; **D.** Normal control, paired worms treated with the AR9 carrier alone.

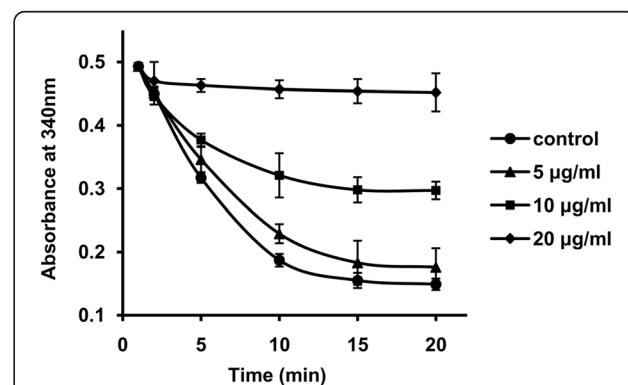


Figure 5 The effect of compound AR9 on rSjAR enzymatic activity. The concentrations of AR9 were 5 µg/ml (triangle), 10 µg/ml (square) and 20 µg/ml (diamond). The AR9 blank was used as a control (circle). The rSjAR concentration in each group was 0.15 µM. The assay was performed independently three times. The background was removed from the data shown here.

The 72 h-dependent LC₅₀ value of AR9 calculated by SPSS 18.0 was 5.72 µg/ml (16.42 µM), with a 95% confidence interval of 4.37 µg/ml-7.91 µg/ml.

Optical images revealed that worms treated with compound AR9 turned black, and obvious damage to the tegument was also observed (Figure 3A and 3B). As a positive control, PZQ induced local drastic contracture, which was consistent with previous studies [28] (Figure 3C). In contrast, these morphological alterations were not observed in the compound-carrier treated group (Figure 3D).

SEM images further confirmed the results of microscopy. Severe wrinkles and extensive small blebs were observed on the tegument layer of AR9-treated worms (Figure 4A and 4B), while PZQ treatment resulted in many ruptures of the tegument layer (Figure 4C). In contrast, the surface of the schistosomes in the control group was very smooth and exhibited a dense network structure (Figure 4D).

Compound AR9 target validation

To verify that *Sj*AR is indeed the target of compound AR9, we assessed the effect of AR9 on *rSj*AR enzymatic activity. A concentration-dependent inhibition of *rSj*AR activity was observed. Compared with the compound-carrier-treated group (0.4% DMSO), AR9 at concentrations of 10 µg/ml and 20 µg/ml reduced *rSj*AR activity by 42.31% and 88.46%, respectively (Figure 5). The half-maximal inhibitory concentration (IC₅₀) calculated by SPSS 18.0 was 11.75 µg/ml (33.72 µM) in the first 10 min, with a 95% confidence interval of 8.87 µg/ml -12.57 µg/ml.

Cytotoxicity assay

To assess the cytotoxicity of compound AR9, three different cell lines (liver carcinoma cells, Hep G2; kidney cells, 293T and breast cells, HeLa) from *H. sapiens* were selected as experimental toxicity screens. For comparison, the activity of all the cells was not significantly affected by exposure to 20 µg/ml of AR9 for 72 h (especially in the Hep G2 cells, where almost no cytotoxicity was observed), while AR9 at 10 µg/ml led to over 90% worm mortality over the same time period (Figure 2 and Figure 6).

Discussion

The antioxidant defense system plays a key role in the physiological functions of an organism [32]. For schistosomes, there have been many studies showing that this system protects the worms from host ROS attack; therefore, the associated enzymes are usually considered to be potential drug-discovery targets [11,33]. *S. japonicum* aldoase reductase, an important enzyme involved in this system, was predicted as a potential drug target. In this study, we firstly obtained the *Sj*AR crystal structure through the X-ray diffraction method, on which a virtual screening and experimental validation strategy was applied

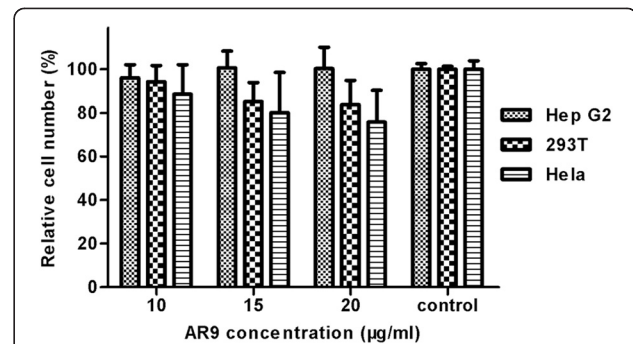
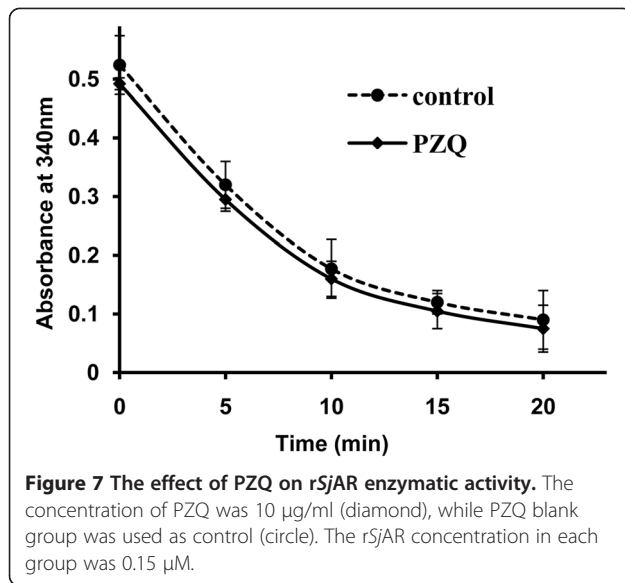


Figure 6 The cytotoxicity of compound AR9 against host cells.

The cell activity of compound-carrier alone treated group was defined as 100%. The relative cell activity values of other experimental groups were calculated by comparing with the control group. The cytotoxicity was determined by Counting Kit-8 analysis, as described in the Methods section.

to screen antischistosomal lead compounds. Finally, one compound, renamed as AR9, was determined to have effective antischistosomal activity but relatively low cytotoxicity towards host cells, which suggested that it has the potential as a lead compound from our selected candidate inhibitors for further drug development.

Although no research has reported the *Sj*AR before, the *Hsa*AR has long been considered to be a potential target for therapies for diabetes and cancer [20,34], and a large number of inhibitors have been identified over the last 30 years. In this study, we also tested the inhibitory activity of two known *Hsa*AR inhibitors (epalrestat and quercetin) on cultured worms, but neither of them exhibited significant activity *in vitro* (data not shown). This may be because of their specificity for targeting *Hsa*AR protein or their failure to reach the target area in schistosomes. In contrast, the compound AR9 exhibited not only a strong inhibition of *rSj*AR enzymatic activity (IC₅₀ =11.75 µg/ml) but also significant inhibitory activity of cultured worms (LC₅₀ =5.72 µg/ml). In this study, we also attempted to obtain the LC₅₀ value of the current drug PZQ for comparison of the corresponding LC₅₀ of AR9. It is of note that although the motor activity of worms exposed to different concentrations of PZQ (1.25 µg/ml-40 µg/ml) decreased significantly in a short time, however, the oral sucker and ventral sucker remained active for a relatively long period, and these worms couldn't be judged as dead according to the death definition described in the Methods section, so we could not provide the accurate LC₅₀ value of PZQ. We acknowledge that the efficacy of AR9 on schistosomes is not as good as PZQ, however, this study is still valuable. As shown in Figure 7, 10 µg/ml of PZQ exhibited no inhibition on *rSj*AR enzymatic activity which indicates that compounds targeting *Sj*AR may have a different mechanism of action compared to PZQ. This result provides the

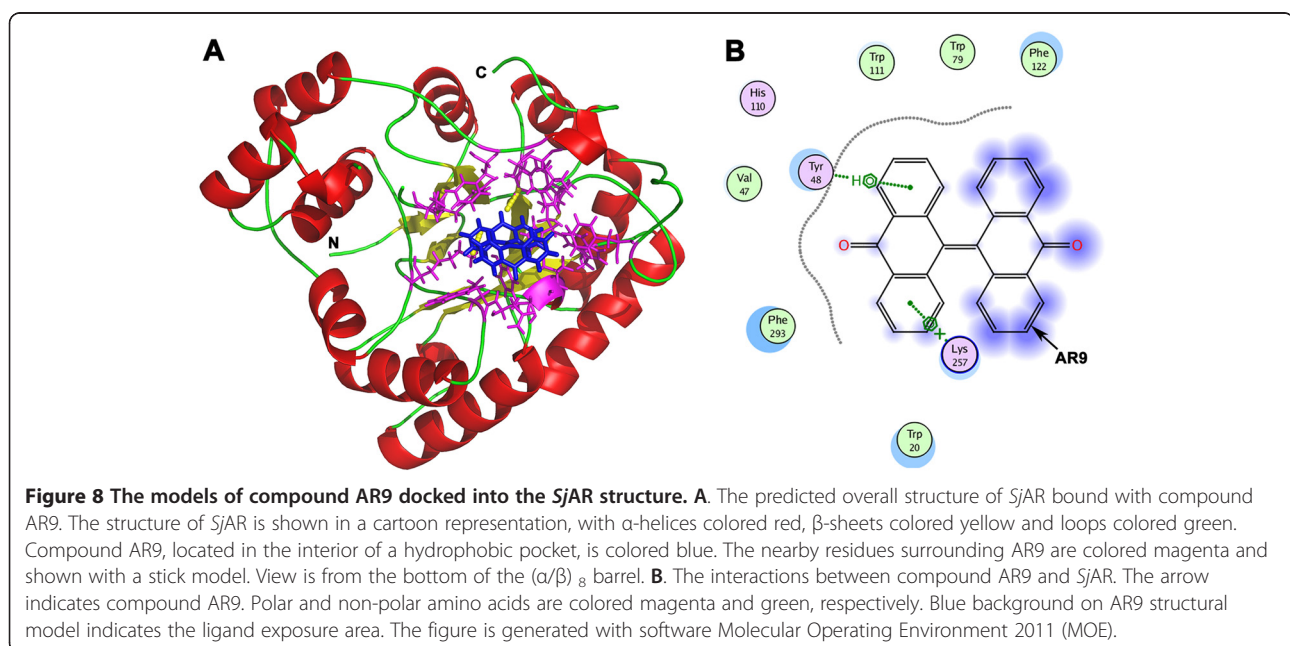


foundation of combination therapy with AR9 and PZQ. Combination therapy is considered to be an effective approach to prevent the emergence of PZQ resistance. The effectiveness of artemisinin derivatives in combination with PZQ has been demonstrated [35]; however, because artemisinin derivatives are effective anti-malaria drugs, there is still concern about the induction of drug-resistant malaria. The results from this study avoid that concern since these compounds have not been used as anti-malarial drugs.

In this study, we also tested the enzyme inhibition for all of the 10 small molecule compounds (Compound

AR8 was not analyzed because of its low solubility) and we tried to find whether there was a positive correlation between enzyme inhibition and parasite growth inhibition. The results showed that, besides AR9, compounds AR1, AR3, AR5 and AR6 also exhibited a certain degree of inhibition on rSjAR enzymatic activity (for AR1, AR3 and AR5, the IC₅₀ values were less than 10 $\mu\text{g/ml}$, while for AR6, the IC₅₀ value was greater than 20 $\mu\text{g/ml}$). However, none of these compounds showed significant inhibitory activity on the cultured worms, except that AR6 resulted in 75% mortality in 72 h at a concentration of 50 $\mu\text{g/ml}$. Therefore, no significant correlation was established between SjAR inhibition and adult worm killing *in vitro*. The reason for this might be explained by other factors, such as compound molecular weight, solubility or their different pharmacokinetics *in vivo*, which could also affect the lack of correlation of the enzyme inhibition assay with activity on cultured worms.

The identified compound, AR9, has two linked anthraquinone scaffolds, and its name is bianthrone or dianthrone. Although anthraquinone scaffolds usually have multiple molecular targets which usually result in their promiscuity, there are indeed some cases that have successfully made the anthraquinone compound into drugs by introducing certain groups. Mitoxantrone, pixantrone and the anthracyclines, all of which are anthraquinone derivatives, have already been used as effective drugs for cancer treatment [36-38]. Additionally, rufigallol, another anthraquinone derivative, also exhibits significant toxic to the malaria parasite *Plasmodium falciparum* [39]. Therefore, although the current structure of AR9 seems unsuitable for a drug, improved derivatives could also be designed



based on this structural model. Additionally, bianthrone is actually the major active ingredient of a widely used Chinese herbal medicine named *rheum palmatum*, which has been demonstrated to effectively inhibit bacteria, fungi and viruses [40,41]. These studies further support the speculation that AR9 has the potential to become a novel antischistosomal lead compound.

Molecular docking analysis showed that AR9 located to the interior of the pocket composed of the residues Val⁴⁷, Tyr⁴⁸, Trp⁷⁹, His¹¹⁰, Trp¹¹¹, Phe¹²², Lys²⁵⁷ and Phe²⁹³. AR9 can bind with the residues Tyr⁴⁸ and Lys²⁵⁷ through the established hydrogen bonds (Figure 8). It is noteworthy that although AR9 has a two-fold symmetry in its scaffold, only one of the anthraquinone moieties interacts with the *SjAR* protein, so the second moiety seems redundant. However, when we removed the other half of the AR9 structure and performed the docking process again, the resulting prototype anthraquinone structure showed poor binding ability with *SjAR* protein. A significant difference was that the previously existing hydrogen bonds between AR9 and *SjAR* protein residues (Tyr⁴⁸ and Lys²⁵⁷) were not established as expected, and meanwhile, no other residues newly-participated in the combination with the prototype anthraquinone. The result might be explained that the second moiety changing the distribution of the electron cloud of the binding regions, thereby facilitating the binding of the first moiety. However, the true binding model between a small molecule and its target protein can only be obtained by analyzing the *SjAR*-AR9 complex structure.

In this study, we have attempted to obtain the crystal structure of *SjAR* complexed with compound AR9 through co-crystallization. However, this was very difficult to achieve because of the relatively lower solubility of AR9. AR9 is soluble in DMSO, but less soluble in water. When the concentration of AR9 in water was higher than 50 µg/ml, some precipitation would occur. Meanwhile, the optimized *SjAR* protein crystallization concentration is 12 mg/ml (approximately 0.31 mM), so even assuming that one *SjAR* protein molecule only binds to one compound molecule, the minimum concentration of AR9 should be 119 µg/ml. However, large amounts of precipitation have already occurred at that concentration. An alternative strategy is to introduce a polar group in the AR9 structure (ensuring that this change does not significantly affect its antischistosomal activity) to increase its solubility, and then attempt co-crystallization.

The majority of previous studies have focused either on the screening and designing of inhibitors of a known drug target or on the analysis of antischistosomal activity of potential drugs [12,42,43], while the work presented here bridges the gap between virtual screening and experimental validation, providing an effective and economical strategy to discover antischistosomal lead compounds. More

work, such as *in vivo* experiments, the design of derivatives and optimization of complex crystallization conditions are still needed in further studies.

Conclusions

The work presented here developed an effective and economical strategy, which integrates virtual screening and experimental validation for the development of new anti-parasitic drugs. In this study, we firstly resolved the *SjAR* structure and identified one compound, bianthrone, which may become a new potential lead compound for developing novel antischistosomal drugs based on this structural model.

Competing interests

The authors declare that they have no competing interests.

Authors' contributions

WH, ZY and XNW conceived and designed the study. JL, DHD, JDC, JPW and SQW performed the experiments, analyzed the data and drafted the manuscript. WH and DHD revised and finalized the manuscript. All of the authors read and approved the final version of the manuscript.

Acknowledgments

The authors thank Que Lan from University of Wisconsin-Madison (USA), Jiahai Zhou from Shanghai Institute of Organic Chemistry, Chinese Academy of Sciences and Hao Ye from East China University of Science and Technology (China) for constructive suggestions about this study. Yanhui Xu, also from Fudan University, is gratefully acknowledged for providing us the facility for protein crystallization. This research was supported by grants from The National Natural Science Foundation of China (grant no. 30400562) and The National Science and Technology Key Project on "Major Infectious Diseases such as HIV/AIDS, Viral Hepatitis Prevention and Treatment" (grant no. 2009ZX10004-302).

Author details

¹Key Laboratory of Parasite and Vector Biology of MOH, Institute of Parasitic Diseases, Chinese Center for Disease Control and Prevention, 207 Rui-Jin Road II, Shanghai 200025, China. ²Department of Microbiology and Microbial Engineering, School of Life Sciences, Fudan University, 220 Han-Dan Road, Shanghai 200433, China. ³Department of Entomology, University of Wisconsin-Madison, 1630 Linden Drive, Madison, WI 53706, USA. ⁴Institutes of Biomedical Sciences, Fudan University, 130 Dong-An Road, Shanghai 200032, China.

Received: 18 December 2012 Accepted: 22 May 2013

Published: 5 June 2013

References

1. Wang L, Utzinger J, Zhou XN: Schistosomiasis control: experiences and lessons from China. *Lancet* 2008, **372**(9652):1793-1795.
2. Mu Y, Huang H, Liu S, Cai P, Gao Y: Molecular characterization and ligand binding specificity of the PDZ domain-containing protein GIPC3 from *Schistosoma japonicum*. *Parasit Vectors* 2012, **5**:227.
3. Chen MG: Use of praziquantel for clinical treatment and morbidity control of schistosomiasis japonica in China: a review of 30 years' experience. *Acta Trop* 2005, **96**(2-3):168-176.
4. Alonso D, Munoz J, Gascon J, Valls ME, Corachan M: Failure of standard treatment with praziquantel in two returned travelers with *Schistosoma haematobium* infection. *Am J Trop Med Hyg* 2006, **74**(2):342-344.
5. Melman SD, Steinauer ML, Cunningham C, Kubatko LS, Mwangi IN, Wynn NB, Mutuku MW, Karanja DM, Colley DG, Black CL, Secor WE, Mkoji GM, Loker ES: Reduced susceptibility to praziquantel among naturally occurring Kenyan isolates of *Schistosoma mansoni*. *PLoS Negl Trop Dis* 2009, **3**(8):e504.
6. Wang W, Dai JR, Li HJ, Shen XH, Liang YS: Is there reduced susceptibility to praziquantel in *Schistosoma japonicum*? Evidence from China. *Parasitology* 2010, **137**(13):1905-1912.

7. Alger HM, Williams DL: The disulfide redox system of *Schistosoma mansoni* and the importance of a multifunctional enzyme, thioredoxin glutathione reductase. *Mol Biochem Parasitol* 2002, **121**(1):129–139.
8. Boumis G, Angelucci F, Bellelli A, Brunori M, Dimastrogiovanni D, Miele AE: Structural and functional characterization of *Schistosoma mansoni* Thioredoxin. *Protein Sci* 2011, **20**(6):1069–1076.
9. Kuntz AN, Davioud-Charvet E, Sayed AA, Califf LL, Dessolin J, Arner ES, Williams DL: Thioredoxin glutathione reductase from *Schistosoma mansoni*: an essential parasite enzyme and a key drug target. *PLoS Med* 2007, **4**(6):e206.
10. Rhee SG, Chae HZ, Kim K: Peroxiredoxins: a historical overview and speculative preview of novel mechanisms and emerging concepts in cell signaling. *Free Radic Biol Med* 2005, **38**(12):1543–1552.
11. Sayed AA, Cook SK, Williams DL: Redox balance mechanisms in *Schistosoma mansoni* rely on peroxiredoxins and albumin and implicate peroxiredoxins as novel drug targets. *J Biol Chem* 2006, **281**(25):17001–17010.
12. Sayed AA, Simeonov A, Thomas CJ, Inglese J, Austin CP, Williams DL: Identification of oxadiazoles as new drug leads for the control of schistosomiasis. *Nat Med* 2008, **14**(4):407–412.
13. Spycher SE, Tabataba-Vakili S, O'Donnell VB, Palomba L, Azzi A: Aldose reductase induction: a novel response to oxidative stress of smooth muscle cells. *FASEB J* 1997, **11**(2):181–188.
14. Srivastava SK, Yadav UC, Reddy AB, Saxena A, Tammali R, Shoeb M, Ansari NH, Bhatnagar A, Petrash MJ, Srivastava S, Ramana KV: Aldose reductase inhibition suppresses oxidative stress-induced inflammatory disorders. *Chem Biol Interact* 2011, **191**(1–3):330–338.
15. Yadav UC, Srivastava SK, Ramana KV: Understanding the role of aldose reductase in ocular inflammation. *Curr Mol Med* 2010, **10**(6):540–549.
16. Vander Jagt DL, Hunsaker LA: Methylglyoxal metabolism and diabetic complications: roles of aldose reductase, glyoxalase-I, betaine aldehyde dehydrogenase and 2-oxoaldehyde dehydrogenase. *Chem Biol Interact* 2003, **143–144**:341–351.
17. Colciago A, Negri-Cesi P, Celotti F: Pathogenesis of diabetic neuropathy—do hyperglycemia and aldose reductase inhibitors affect neuroactive steroid formation in the rat sciatic nerves? *Exp Clin Endocrinol Diabetes* 2002, **110**(1):22–26.
18. Kang ES, Iwata K, Ikami K, Ham SA, Kim HJ, Chang KC, Lee JH, Kim JH, Park SB, Yabe-Nishimura C, Seo HG: Aldose reductase in keratinocytes attenuates cellular apoptosis and senescence induced by UV radiation. *Free Radic Biol Med* 2011, **50**(6):680–688.
19. Rath J, Gowri VS, Chauhan SC, Padmanabhan PK, Srinivasan N, Madhubala R: A glutathione-specific aldose reductase of *Leishmania donovani* and its potential implications for methylglyoxal detoxification pathway. *Gene* 2009, **429**(1–2):1–9.
20. Tammali R, Saxena A, Srivastava SK, Ramana KV: Aldose reductase regulates vascular smooth muscle cell proliferation by modulating G1/S phase transition of cell cycle. *Endocrinology* 2010, **151**(5):2140–2150.
21. Doudna JA, Grosshans C, Gooding A, Kundrot CE: Crystallization of ribozymes and small RNA motifs by a sparse matrix approach. *Proc Natl Acad Sci U S A* 1993, **90**(16):7829–7833.
22. Otwinowski Z, Minor W: Processing of X-ray diffraction data collected in oscillation mode. *Macromol Crystall Pt A* 1997, **276**:307–326.
23. McCoy AJ, Grosse-Kunstleve RW, Storoni LC, Read RJ: Likelihood-enhanced fast translation functions. *Acta Crystallogr D: Biol Crystallogr* 2005, **61**(Pt 4):458–464.
24. Emsley P, Cowtan K: Coot: model-building tools for molecular graphics. *Acta Crystallogr D: Biol Crystallogr* 2004, **60**(Pt 12 Pt 1):2126–2132.
25. Adams PD, Grosse-Kunstleve RW, Hung LW, Ioerger TR, McCoy AJ, Moriarty NW, Read RJ, Sacchettini JC, Sauter NK, Terwilliger TC: PHENIX: building new software for automated crystallographic structure determination. *Acta Crystallogr D: Biol Crystallogr* 2002, **58**(Pt 11):1948–1954.
26. Xiao SH, Mei JY, Jiao PY: The *in vitro* effect of mefloquine and praziquantel against juvenile and adult *Schistosoma japonicum*. *Parasitol Res* 2009, **106**(1):237–246.
27. Djoubissie PO, Snirc V, Sotnikova R, Zurova J, Kyselova Z, Skalska S, Gajdosik A, Javorkova V, Vlkovicova J, Vrbjar N, Stefek M: *In vitro* inhibition of lens aldose reductase by (2-benzyl-2,3,4,5-tetrahydro-1H-pyrido [4,3-b]indole-8-yl)-acetic acid in enzyme preparations isolated from diabetic rats. *Gen Physiol Biophys* 2006, **25**(4):415–425.
28. Portela J, Boissier J, Gourbal B, Pradines V, Colliere V, Cosledan F, Meunier B, Robert A: Antischistosomal activity of trioxaquines: *In vivo* efficacy and mechanism of action on *Schistosoma mansoni*. *PLoS Negl Trop Dis* 2012, **6**(2):e1474.
29. Ferrell M, Abendroth J, Zhang Y, Sankaran B, Edwards TE, Staker BL, Van Voorhis WC, Stewart LJ, Myler PJ: Structure of aldose reductase from *Giardia lamblia*. *Acta Crystallogr Sect F Struct Biol Cryst Commun* 2011, **67**(Pt 9):1113–1117.
30. Gallego O, Ruiz FX, Ardevol A, Dominguez M, Alvarez R, de Lera AR, Rovira C, Farres J, Fita I, Pares X: Structural basis for the high all-trans-retinaldehyde reductase activity of the tumor marker AKR1B10. *Proc Natl Acad Sci U S A* 2007, **104**(52):20764–20769.
31. Zhao HT, Soda M, Endo S, Hara A, El-Kabbani O: Selectivity determinants of inhibitor binding to the tumour marker human aldose reductase-like protein (AKR1B10) discovered from molecular docking and database screening. *Eur J Med Chem* 2010, **45**(9):4354–4357.
32. Krauth-Siegel RL, Leroux AE: Low-molecular-mass antioxidants in parasites. *Antioxid Redox Signal* 2012, **17**(4):583–607.
33. Guevara-Flores A, Pardo JP, Rendon JL: Hysteresis in thioredoxin-glutathione reductase (TGR) from the adult stage of the liver fluke *Fasciola hepatica*. *Parasitol Int* 2011, **60**(2):156–160.
34. Kawai T, Takei I, Tokui M, Funae O, Miyamoto K, Tabata M, Hirata T, Saruta T, Shimada A, Itoh H: Effects of epalrestat, an aldose reductase inhibitor, on diabetic peripheral neuropathy in patients with type 2 diabetes, in relation to suppression of N(varepsilon)-carboxymethyl lysine. *J Diabetes Complications* 2010, **24**(6):424–432.
35. Angelucci F, Basso A, Bellelli A, Brunori M, Pica Mattoccia L, Valle C: The anti-schistosomal drug praziquantel is an adenosine antagonist. *Parasitology* 2007, **134**(Pt 9):1215–1221.
36. Jamal-Hanjani M, Pettengell R: Pharmacokinetic evaluation of pixantrone for the treatment of non-Hodgkin's lymphoma. *Expert Opin Drug Metab Toxicol* 2011, **7**(11):1441–1448.
37. Minotti G, Menna P, Salvatorelli E, Cairo G, Gianni L: Anthracyclines: molecular advances and pharmacologic developments in antitumor activity and cardiotoxicity. *Pharmacol Rev* 2004, **56**(2):185–229.
38. Montazerabadi AR, Szargania A, Bahreyni-Toosi MH, Ahmadi A, Shakeri-Zadeh A, Aledavood A: Mitoxantrone as a prospective photosensitizer for photodynamic therapy of breast cancer. *Photodiagnosis Photodyn Ther* 2012, **9**(1):46–51.
39. Winter RW, Cornell KA, Johnson LL, Ignatushchenko M, Hinrichs DJ, Riscoe MK: Potentiation of the antimalarial agent rufigallol. *Antimicrob Agents Chemother* 1996, **40**(6):1408–1411.
40. Sun SW, Yeh PC: Analysis of rhubarb anthraquinones and bianthrone by microemulsion electrokinetic chromatography. *J Pharm Biomed Anal* 2005, **36**(5):995–1001.
41. Wang J, Zhao H, Kong W, Jin C, Zhao Y, Qu Y, Xiao X: Microcalorimetric assay on the antimicrobial property of five hydroxyanthraquinone derivatives in rhubarb (*Rheum palmatum* L.) to *Bifidobacterium adolescentis*. *Phytomedicine* 2010, **17**(8–9):684–689.
42. Postigo MP, Guido RV, Oliva G, Castilho MS, da RPI, de Albuquerque JF, Andricopulo AD: Discovery of new inhibitors of *Schistosoma mansoni* PNP by pharmacophore-based virtual screening. *J Chem Inf Model* 2010, **50**(9):1693–1705.
43. Marxer M, Ingram K, Keiser J: Development of an *in vitro* drug screening assay using *Schistosoma haematobium* schistosomula. *Parasit Vectors* 2012, **5**:165.

doi:10.1186/1756-3305-6-162

Cite this article as: Liu et al.: Aldose reductase from *Schistosoma japonicum*: crystallization and structure-based inhibitor screening for discovering antischistosomal lead compounds. *Parasites & Vectors* 2013 **6**:162.